SECOND EUROPEAN CONFERENCE ON EARTHQUAKE ENGINEERING
AND SEISMOLOGY, ISTANBUL AUG. 25-29, 2014

QUASI-STATIC CYCLIC TESTS ON U-SHAPED REINFORCED CONCRETE WALLS SUBJECTED TO DIAGONAL LOADING

Raluca CONSTANTIN[1] and Katrin BEYER[2]

ABSTRACT

This article presents the test setup of two quasi-static cyclic tests on U-shaped walls under horizontal diagonal loading recently performed at EPF Lausanne. The results of the first test are discussed in terms of global behaviour: failure mechanisms and force-displacement hystereses as well as in terms of local behaviour. The emphasis is placed on behaviour specific to U-shaped walls under diagonal loading, such as: 1) proneness to out-of-plane buckling of the free ends of the flanges; and 2) plane sections do not remain plane after deformation. Implications of these phenomena in the design and analysis of U-shaped walls are also discussed.

INTRODUCTION

Reinforced concrete (RC) core walls are often used to brace mid- to high-rise buildings. Due to the core wall's geometry (e.g. T-shaped, U-shaped, L-shaped wall sections) they provide strength and stiffness in both horizontal directions leading to a rather complex seismic behaviour. One of the simplest types of core wall is the wall with a U-shaped section. Previous experimental campaigns on U-shaped walls (Reynouard and Fardis, 2001; Beyer et al., 2008; Lowes et al., 2013) have shown the complex behaviour such walls especially under bidirectional loading. The diagonal loading direction has been identified as a particular critical one (Beyer et al., 2008), with the experimental maximum moment capacity being significantly overestimated by plastic hinge analysis.

With the objective to better understand the behaviour of U-shaped walls under diagonal loading and to complement the scarce experimental data on such walls, a new testing campaign was carried out at the structural engineering laboratories at the EPF Lausanne. The experimental campaign included the quasi-static cyclic testing of two half-scale U-shaped walls under bending along the two geometric diagonals of the U-shaped section. Parameters investigated were: the axial load ratio and the vertical reinforcement layout.

This article presents first the test setup of the two walls, including the instrumentation and the loading protocol. Second, the test results for the first wall are presented in terms of global behaviour such as: force-displacement hystereses and failure mechanisms. Third, selected local behaviour quantities, such as vertical strains at the wall base are shown. Finally, conclusions for the analysis and design of U-shaped walls are discussed.

[1] PhD student, Earthquake Engineering and Structural Dynamics Laboratory (EESD), School of Architectural, Civil and Environmental Engineering (ENAC), École Polytechnique Fédérale de Lausanne (EPFL), Switzerland
[2] Assistant Professor, Earthquake Engineering and Structural Dynamics Laboratory (EESD), School of Architectural, Civil and Environmental Engineering (ENAC), École Polytechnique Fédérale de Lausanne Switzerland

TEST SETUP

The test campaign is a continuation of the tests performed on U-shaped walls in ETH Zurich by Beyer et al. (2008), hence the test setups are rather similar. Therefore, the present paper will mainly emphasise the differences between the two test campaigns while for further details on the test setup the reader is referred to Beyer et al. (2008).

Both test units of the new test campaign, named TUC (Test Unit C) and TUD (Test Unit D) were identical with regard to section dimensions, vertical reinforcement layout and confining reinforcement layout. The wall dimensions and the reinforcement layout for the two test units are shown in Figure 1 while a photo of the test setup is shown in Figure 2a.

As it can be seen from Figure 1a, both walls had one flange detailed with vertical reinforcement mainly concentrated in the boundary elements while the other flange and the web were both detailed with vertical reinforcement uniformly distributed along the length of the wall sections. The amount of uniformly distributed reinforcement was chosen in order to obtain equal moment capacities of the wall in the corresponding diagonal directions, namely equal moment capacity for positions E and H and respectively for positions F and G. The varying parameter between the two tests was the axial load ratio. While TUC had an axial load ratio of 0.06, TUD was subjected to an axial load ratio of 0.15.

Similarly to Beyer et al. (2008), the walls were loaded horizontally with three actuators: the EW actuator loaded the web at a height of h=3.35m while the NS actuators loaded the flanges of the wall at a height of h=2.95 from the foundation, as shown in the photo of the test setup (Figure 2a). The test was performed in displacement control and the rotation at the top of the wall was restrained by imposing at all times equal top displacements with the NSE and NSW actuators. The axial load was applied by a tendon pre-tensioned with a hollow core jack and was kept constant throughout the tests.

The wall behaviour was monitored during testing though conventional measurement systems (linear variable differential transducers (LVDTs) and load cells), an optical measurement system based on triangulation of active LEDs, photos, manual measurements of cracks and hand notes. Figure 3 shows a sketch of the two measurement systems as well as of the cardinal system used as reference system for forces and displacements. LVDTs were used to measure global horizontal displacements at the top of the wall as well as vertical elongation of the wall edges with four chains of eight LVDTs each mounted on the outer side of the wall along the edges. This measurement construction is the same as the one used by Beyer et al. (2008). In addition two other chains of four LVDTs were added on the inner side of each of the flange end to capture any vertical strain variation through the thickness of the flange end.

The optical measurement system, called Optotrak Certus (NDI, 2009), was composed of markers and optical cameras recording the markers x, y, z positions. The markers were glued on the outer side of the wall in regular grids of 100x125mm (TUC) and 100x100 (TUD) to match spacing of horizontal and longitudinal bars. One additional row of markers was placed on the foundation of the wall to record any sliding or uplift displacements. The height of the marker grid was limited to ~1.7m above the foundation as the main interest was to capture the plastic hinge zone of the wall while respecting the measurement volume of the optical measurement system.

The material properties the reinforcement and the concrete used for the construction of TUC are shown in Table 1 and Table 2. Concrete properties from material tests: concrete compressive strength f'_c, concrete elastic modulus E_c and the concrete tensile strength f'_t correspond to properties at the day of testing, except the f'_c - *28days*, which corresponds to the concrete compressive strength on cylinder at 28 days. The yield strength f_y, the ultimate strength f_u and the ultimate strain ε_{su} of the reinforcement bars are given in Table 2 and correspond to properties at day of testing. Additionally for the D12 bars, the hardening strain is given, which marks the end of the constant strength hardening plateau and beginning of increasing strength hardening zone. With values of f_u/f_y between 1.18 and 1.32, all reinforcement bars correspond to “Class C” grade according to Eurocode 8 (CEN, 2004).

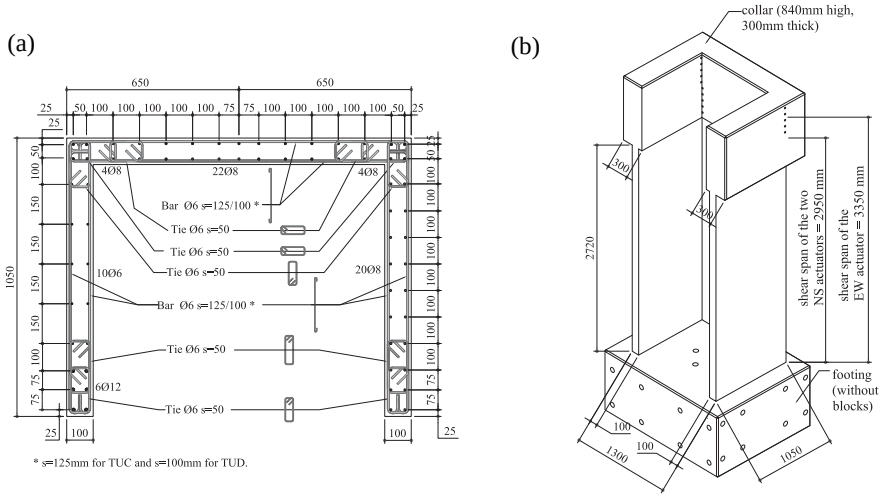

Figure 1 TUC and TUD geometry: cross-section (a) and elevation (b)

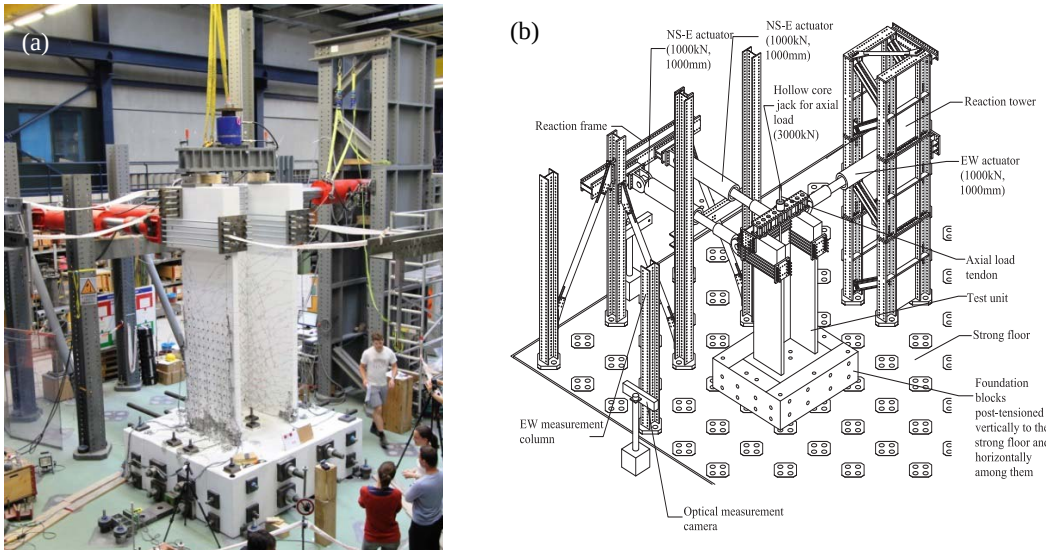

Figure 2 Photo of the test setup in the structural engineering laboratory at EPF Lausanne (a) and sketch of the test setup (b)

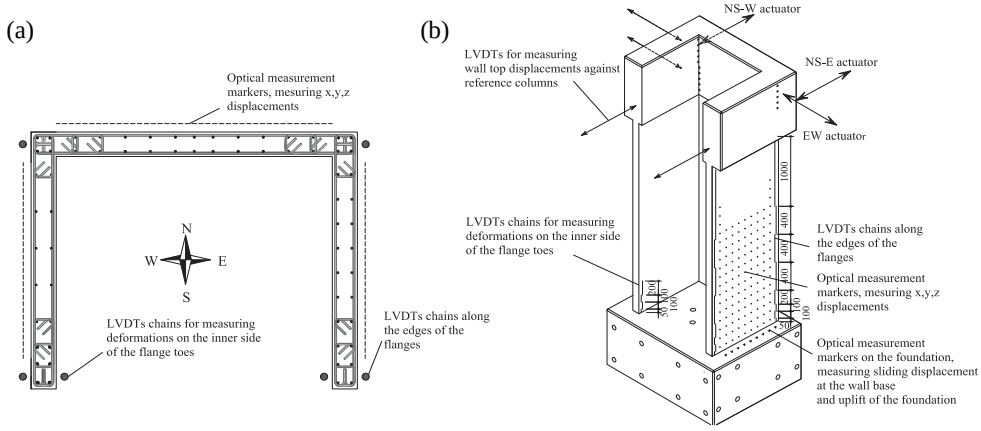

Figure 3 Instrumentation of the test units: cross-section view (a) and elevation (b)

The loading protocol focused on the diagonal loading direction (Figure 4b). Cycles along the principle directions were added at small drift levels in order to check the strength capacity of the wall in these directions, for which the strength can be predicted well based on the plane section hypothesis. The standard loading protocol for both test units is shown below.

- 0.1% drift: O→C→D→O→A→B→O
- 0.2% drift: O→C→D→O→A→B→O→E→F→O→H→G→O
- 0.3%, 0.4%, 0.6% drifts: O→E→F→O→H→G→O→C→D→O→A→B→O
- 0.8% drift: O→C→D→C→D→O→A→B→A→B→O
- 1.0%, 2.0%, 3.0% drifts: O→E→F→E→F→O→H→G→H→G→O
- 1.5%, 2.5% drifts: O→H→G→H→G→O→E→F→E→F→O

Starting with 1.0% drift, two complete reverse cycles were applied at each diagonal direction and drift level. The orientation of the first diagonal applied at a new drift level was alternated between the E-F direction and the H-G direction. Towards the end of the tests the loading protocol for TUC was modified due to extensive damage to the East flange toe. In order to minimize the effect of the order of cycling in the two diagonals on the wall behaviour, the loading protocol was modified as follows:

- 2.5% drift: O→H→G→O→ E→F→ O
- 3.0% drift: O→E→O→H→O (test was stopped due to initiation of loss of vertical load bearing capacity)

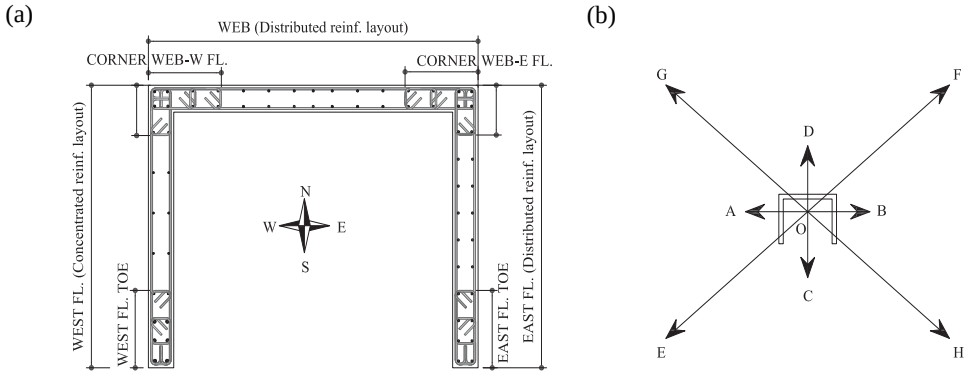

Figure 4 Cardinal positions for wall reference (a) and loading positions (b)

Table 1 Properties of the reinforced concrete used for the construction of TUC

	f'_c - *28days* [MPa]	f'_c [MPa]	E_c [GPa]	f'_t [MPa]
TUC	38.1	42.0	31.6	3.20

Table 2 Properties of the reinforcement bars used for the construction of TUC

	f_y [MPa]	f_u [MPa]	f_u/f_y [-]	ε_{sh} [%]	ε_{su} [%]
D6mm bars	492	623	1.27	-	7.2
D8mm bars	563	663	1.18	-	8.2
D12mm bars	482	636	1.32	2.7	12.6

TEST RESULTS

The experimental results are presented here only for the first test unit TUC. Global results are given in terms of failure mechanism and force-displacement hystereses. To characterise the local behaviour, vertical strains at the base of the wall and at the inner and outer side of the flange toes are presented. Further results as well as those of TUD are included in Constantin and Beyer (2014).

Global results

Failure of TUC is described with the help of photos (Figure 5 and Figure 6), with force-displacement hystereses of individual actuators as well as with SRSS force-displacement hystereses (Figure 7 and Figure 8). The SRSS quantities are defined as follows:

$$F_{SRSS} = \sqrt{{M_{EW}}^2 + {M_{NS}}^2} * sign(\Delta_{NS})/h_{NS} \quad (1)$$

$$\Delta_{SRSS} = \sqrt{\left({\Delta_{NS}}^2 + {\Delta_{EW@2.95}}^2\right)} * sign(\Delta_{NS}) \quad (2)$$

TUC failed due to out-of-plane buckling of the West flange toe, upon loading to position E with a target drift of 3.0% (Figure 5). The last loading cycle to position E had the loading branch marked by a very reduced stiffness and reached only 1.5% drift before a strength drop of 50% in the SRSS force (Figure 8a). The reduction of the loading stiffness is due to the fact that the buckling of the boundary element of the West flange had already initiated upon load reversal from position F at 2.5% drift to zero displacement.

Out-of-plane buckling of the flange toe was promoted by the diagonal loading in the E-F direction which acted as in-plane and out-of-plane loading for the flange. The diagonal loading pattern led to a variation of the vertical strains at the base of the flange toe between the two sides of the wall: inner side and outer side as shown in Figure 9. The outer side of the flange toe underwent higher tensile strains compared to the inner side when loading to position F but also the higher absolute compression strains when returning to position E.

Although failure of the wall was reached with the out-of-plane buckling of the West flange, loading was continued according to the modified loading protocol since the wall still possessed significant stiffness in the H-G diagonal and could still carry the vertical load. The East flange failed due to compression failure of the unconfined concrete part (Figure 6) after significant damage in the previous loading cycles to the boundary element. Failure occurred at 2.5% when loading to position H (Figure 7e-h and Figure 8b). The boundary element of the East flange underwent bar buckling at an earlier drift than the West flange due to same confinement reinforcement but smaller bar diameter (Restrepo, 1993). Bar buckling led to bar fractures (Figure 7e-h and Figure 8b) and expedited concrete crushing in the East flange toe. However the fracture of the three bars in the boundary element did not mark the failure of the wall since it led only to a 15% decrease in the SRSS force capacity with respect to the maximum previously attained force. The relatively low drop in force capacity is due to the uniform distribution of the D8 bars in the East flange.

It is believed that the different failure modes of the two flanges were also influenced by the vertical reinforcement layout. As pointed out by Rosso et al. (2014) based on works by Pauley and Priestley (1993) and Chai and Elayer (1999), out-of-plane buckling of a wall is influenced by the mechanical reinforcement ratio of the vertical reinforcement in the boundary element. The larger is the mechanical reinforcement ratio (as in the case of concentrated reinforcement layout) the lower are the maximum tensile strains that need to be reached in previous loading cycles for out-of-plane buckling to occur.

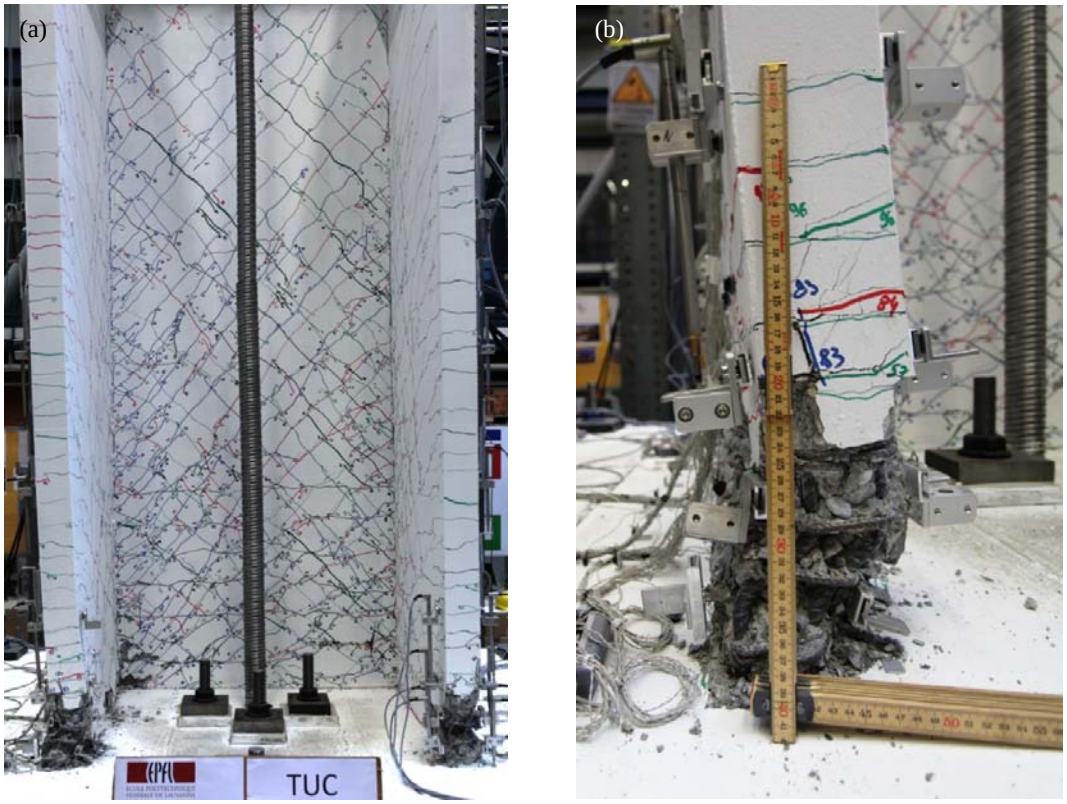

Figure 5 TUC failure at 1.5% drift during loading to position E: out-of-plane buckling and compression failure of the concentrated reinforcement flange. Front view (a) and detailed view of the damaged flange toe (b)

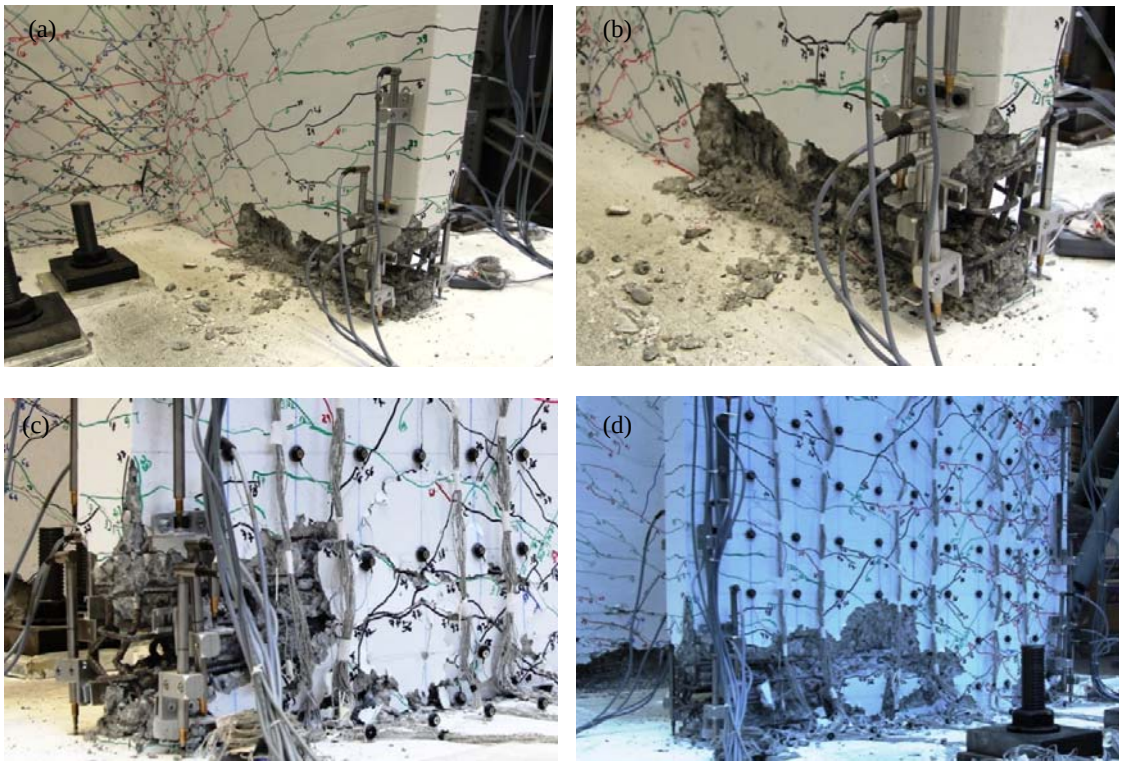

Figure 6 TUC: Compression crushing failure of the concrete in the East flange. Loading to position H, target drift δ=3.0%. Inside view: general (a) and close-up (b) and outside view: general (c) and close-up (d)

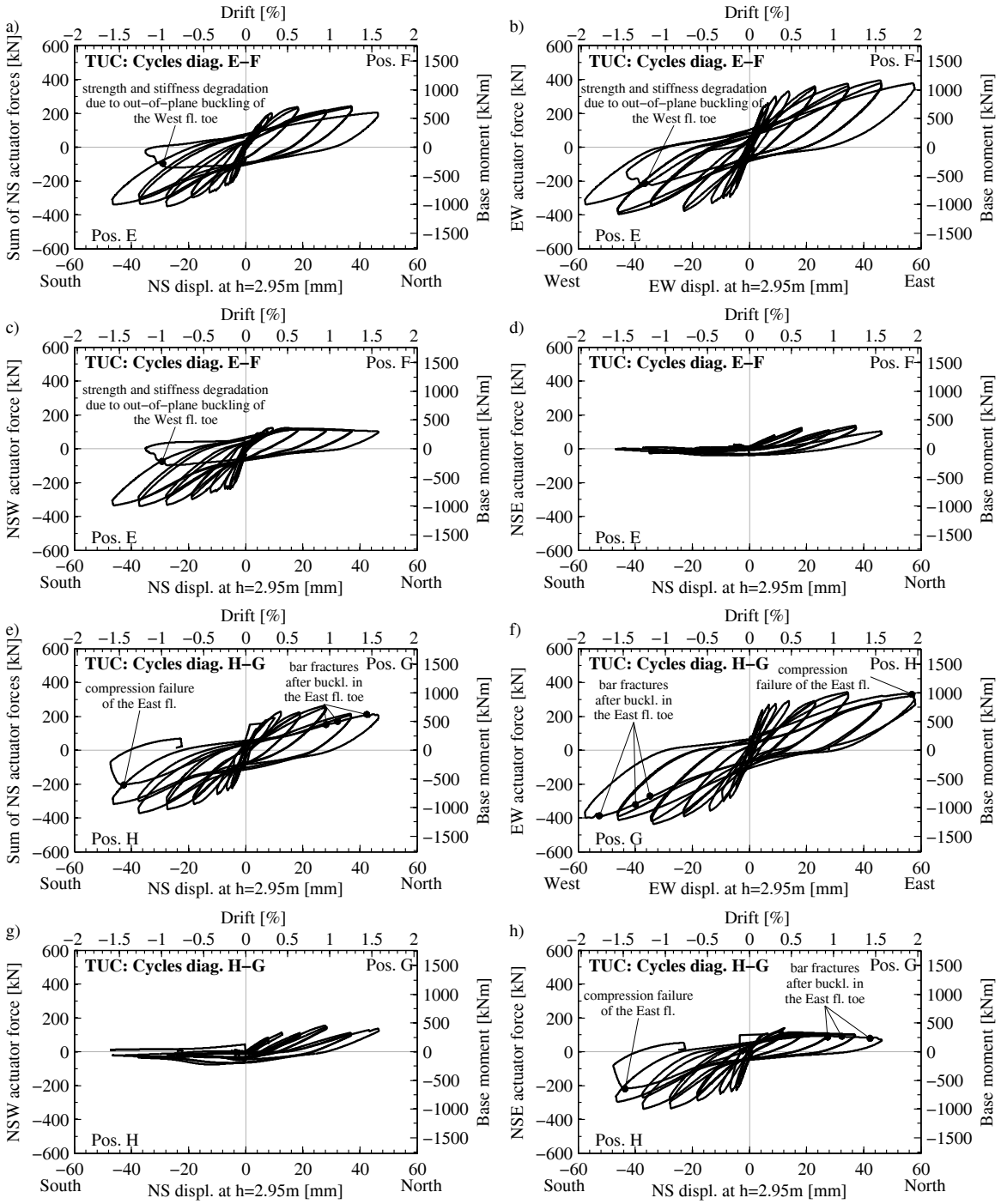

Figure 7 TUC: force-displacement hystereses of individual actuators

Local deformation results

The local deformation results for TUC are presented here in terms of vertical strains on the inner and the outer side of the flange ends (Figure 9) and vertical strains at the base of the wall (Figure 10).The vertical strains at the flange ends on the inner side and the outer side of the wall were obtained from LVDT measurements at *h*=50-850mm above the foundation. The vertical strains at the base of the wall

were obtained for the outer side of the wall from optical measurements. Strains at the base of the wall were computed from the first row of markers on the wall and from the row the markers on the foundation.

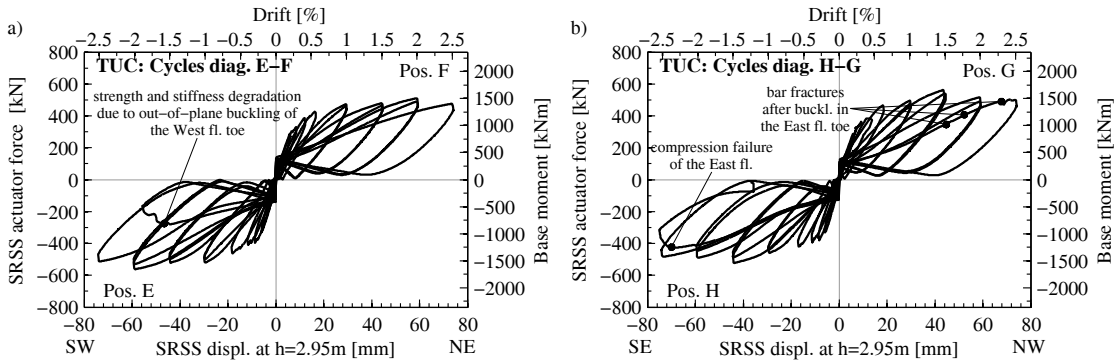

Figure 8 TUC: SRSS force-displacement hystereses for the diagonal loading directions

The vertical strains on both sides of the flange toes are shown for the East flange at positions H and G and for the West flange at positions E and F (Figure 9). For each of the two flanges, these are the loading positions which impose the largest tensile and compressive strains on the toes. Strains are plotted for two different drifts: 0.4% representing a drift level close to yield drifts under diagonal loading and 1.0% representing a drift level in the inelastic range. It can be observed that the compressive strains on the outer side of the toes are larger than on the inner side when the flange toe comes under compression (Figure 9a-b) but also the tensile strains are larger in the outer side of the wall than in the inner side when the flange toes are in tension (Figure 9c-d). This behaviour is specific to diagonal loading due to geometrical considerations and it creates the potential for out-of-plane buckling of the flange toes due to the difference in inelastic strains imposed on the two sides of the flange toe.

The vertical strains at the base of the wall under diagonal loading positions are shown in Figure 10, again for two drifts: 0.4% and 1.0%. From Figure 10a and c, when the East flange comes in compression at position H and the West flange at position E, the vertical strain at the base along the length of the flanges is nonlinear with compression strain peaks at the flange toe but also at the corner between flange and web. Additionally, at positions F and G, vertical strains at the base along the length of the web are again nonlinear. Both observations indicate that plane sections do not remain plane after deformations since the vertical strain profiles are nonlinear over individual wall sections.

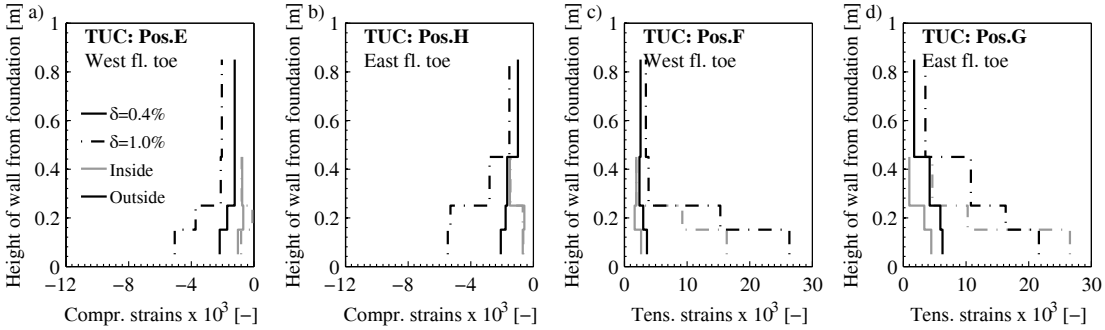

Figure 9 TUC: vertical strains at the toe of the flanges under diagonal loading from LVDT measurements - comparison between strains on the inner side and on the outer side of the wall

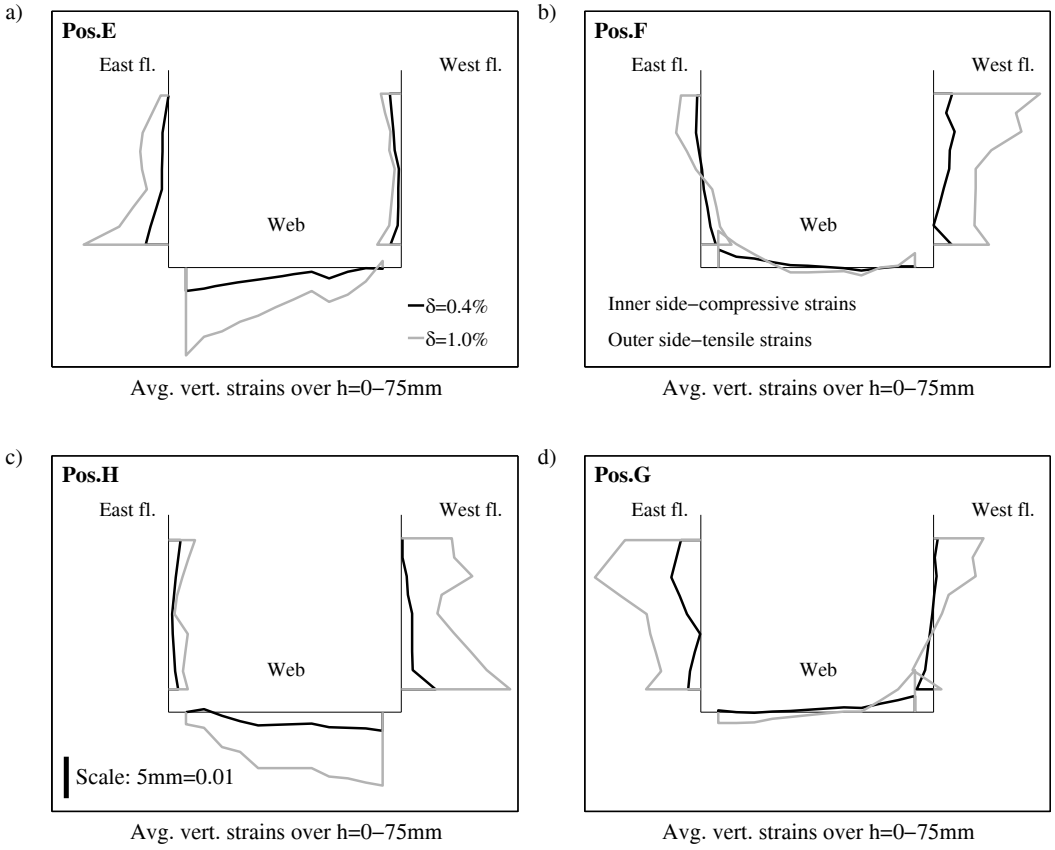

Figure 10 TUC: vertical strains at the base of the wall under diagonal loading directions obtained from optical measurements averaged over the h=0-75mm above foundation: view of the wall cross-section

CONCLUSIONS

The article presents the test setup of two quasi-static cyclic tests on U-shaped walls subjected to diagonal loading. The results of the first test (TUC) were presented in terms of global as well as local results. TUC failed due to out-of-plane buckling of the flange toe, and it was shown that U-shaped walls are prone to such a failure mechanism under the diagonal loading pattern. Consideration should be hence given in the design of U-shaped walls to minimising the potential for out-of-plane buckling of the flange toes especially when large inelastic deformations are expected. One way this can be achieved is with a distributed vertical reinforcement layout and in this case attention should be given to the necessary confinement lengths which will increase as compared to the concentrated reinforcement layout.

One other observed behaviour of U-shaped walls under diagonal loading is that the plane section assumption does not hold. The vertical strains are nonlinear at the base of the wall for the U-shaped section for the individual rectangular wall sections considered separately. This means that analysis methods based on plane section analysis, such as plastic hinge analysis, do not apply to U-shaped walls under diagonal loading directions or only apply with certain limitations. Current work focuses on the definition of these limitations as well as the development of plastic hinge length equations for U-shaped walls and the validation of approaches for incorporating shear deformations in ultimate displacement estimates derived from plastic hinge approaches (Beyer et al., 2011).

REFERENCES

Beyer K, Dazio A, Priestley MJN (2008) "Quasi-static cyclic tests of two U-shaped reinforced concrete walls", *Journal of Earthquake Engineering* 12 (7), 1023-1053

Beyer K, Dazio A, Priestley MJN (2011) "Shear deformations of slender reinforced concrete walls under seismic loading," *ACI Structural J*. 108(2): 167-177

Chai YH, Elayer DT (1999) "Lateral Stability of Reinforced Concrete Columns under Axial Reversed Cyclic Tension and Compression", *ACI Structural Journal* 96(5):780-790

Constantin R, Beyer K (2014) "Behaviour of U-shaped reinforced concrete walls subjected to quasi-static cyclic tests under diagonal loading", *Engineering Structures*, to be submitted

CEN Eurocode 8 (2004): Design provisions for earthquake resistance of structures, Part 1: General rules, seismic actions and rules for buildings EN 1998-1:2004, Brussels (Belgium): European Committee for Standardisation

NDI (2009). Optotrak Certus HD, Northern Digital Inc. Waterloo, Ontario (Canada); http://www.ndigital.com/industrial/certushd.php;

Paulay T, Priestley JN (1993) "Stability of Ductile Structural Walls", *ACI Structural Journal* 90(4):385-392

Restrepo-Posada JI (1993) Seismic behaviour of connections between precast concrete elements. Ph.D. Thesis, 93-3, Department of Civil Engineering, University of Canterbury, Christchurch, New Zeeland

Reynouard JM and Fardis MN, Eds (1993) Shear wall structures, ECOEST/ICONS Thematic Report No5, LNEC-National Laboratory of Civil Engineering, Lisbon, Portugal

Rosso A, Almeida J, Constantin R, Beyer K, Sritharan S (2014) "Influence of longitudinal reinforcement layouts on RC wall performance", *Proceedings of the Second European Conference on Earthquake Engineering and Seismology*, Istanbul, Turkey, 24-29 August

Lowes L, Lehman D, Kuchma D, Mock A, Behrouzi A (2013) Large scale tests of C-shaped reinforced concrete walls. Summary report, NEES project warehouse; https://nees.org/warehouse/project/104